THE JOURNAL OF BIOLOGICAL CHEMISTRY
Vol. 276, No. 17, Issue of April 27, pp. 14385–14392, 2001
Printed in U.S.A.

Tumor Targeting of Mono-, Di-, and Tetravalent Anti-p185^{HER-2} Miniantibodies Multimerized by Self-associating Peptides*

Received for publication, December 26, 2000
Published, JBC Papers in Press, January 22, 2001, DOI 10.1074/jbc.M011669200

Jörg Willuda‡§¶, Susanne Kubetzko‡§, Robert Waibel‖, P. August Schubiger‖, Uwe Zangemeister-Wittke§, and Andreas Plückthun‡**

From the ‡Department of Biochemistry, University of Zürich, CH-8057 Zürich, §Division of Oncology, Department of Internal Medicine, University Hospital, CH-8044 Zürich, and ‖Center of Radiopharmaceutical Science, Paul Scherrer Institute, CH-5232 Villigen (PSI), Switzerland

Multimerization of antibody fragments increases the valency and the molecular weight, both identified as key features in the design of the optimal targeting molecule. Here, we report the construction of mono-, di-, and tetrameric variants of the anti-tumor p185^{HER-2} single chain Fv fragment 4D5 by fusion of self-associating peptides to the carboxyl terminus. Dimeric miniantibodies with a synthetic helix-turn-helix domain and tetrameric ones with the multimerization domain of the human p53 protein were produced in functional form in the periplasm of *Escherichia coli*. We have directly compared these molecules and the single-chain Fv fragment in the targeting of SK-OV-3 xenografts. Tetramerization of the 4D5 antibody fragment resulted in increased serum persistence, significantly reduced off-rate, due to the avidity effect, both in surface plasmon resonance measurements on purified p185^{HER-2} and on SK-OV-3 cells. The ^{99m}technetium-tricarbonyl-labeled tetrameric 4D5-p53 miniantibody localized with the highest dose at the tumor and remained stably bound for at least 72 h. The highest total dose was 4.3% injected dose/g after 24 h, whereas the highest tumor-to-blood ratio was found to be 13.5:1 after 48 h, with a total dose of 3.2% injected dose/g. The tetramer shows no higher avidity than the dimer, presumably since the simultaneous binding to more than two antigen molecules on the surface of cells is not possible, and the improvement in performance over the dimer must at least be due in part to the molecular weight. These results demonstrate that multimerization by self-associating peptides can be used for the development of more effective targeting molecules for medical diagnostics and therapy.

One of the current visions in the medical application of recombinant antibody technology (1) is the specific targeting and delivery of effector agents such as radioisotopes, toxins, or enzymes to tumors or other disease-related sites in the body. Unfortunately, recombinant antibody fragments have exhibited poor *in vivo* targeting efficiency, probably due to their fast clearance from the blood circulation resulting in low total dose accumulation (2–4). The targeting efficacy of antibody fragments can be improved by the use of multimeric formats of antibody fragments with higher avidity and a molecular weight slightly above the renal filtration threshold (5–7). This has first been shown in studies in which Fab and scFv[1] fragments were multimerized by chemical linkage (8–12). More efficient is the multimerization of antibody fragments by modification of the polypeptide sequence itself by recombinant DNA technology and the subsequent purification of the multimeric protein from the bacterial host. One strategy is to shorten the flexible peptide linker of scFv fragments to make it impossible to form monomers (5, 13). The so-called "diabodies" have been shown to be stable under *in vivo* conditions and to enrich efficiently at xenografts (14, 15). Another strategy is the fusion of the homodimerization domain C_H3 to the carboxyl terminus of the polypeptide chain. By using this approach in combination with a stabilizing intramolecular disulfide bridge for an anti-carcinoembryonic antigen scFv fragment, very promising tumor targeting data were reported (7). However, recombinant molecules that contain additional disulfide bridges are usually produced at lower yields in heterologous expression systems and are generally less convenient to handle (16).

Instead of using whole protein domains self-associating peptides can be used as multimerization modules to form so-called miniantibodies (6). Here we report on the engineering and production of mono-, di-, and tetrameric variants of the anti-p185^{HER-2} scFv fragment 4D5 in the periplasm of *Escherichia coli* and their *in vivo* application for targeting xenografted SK-OV-3 tumors. The comparison of the various formats is expected to provide insight into the performance of such multimerized molecules for *in vivo* targeting purposes and serve as a proof of this concept under *in vivo* conditions. We demonstrate that the *in vivo* stability of the tetrameric miniantibody is high enough to result in efficient tumor targeting and that such multimerized antibody fragments can be readily produced in the periplasm of *E. coli* (17, 18) and be used to deliver radionuclides or other effector molecules for imaging and therapy.

MATERIALS AND METHODS

Mammalian Cell Lines and Recombinant Antigen—The breast carcinoma cell line SK-BR-3 (HTB 30, ATCC, Rockville MD) and the ovarian carcinoma cell line SK-OV-3 (HTB 77, ECACC, Salisbury, Wilts, UK) were maintained in McCoy's 5A medium (Amimed BioConcept, Pillschwill, Switzerland), supplemented with 15% bovine serum (Life Technologies, Inc.). For binding experiments the adherent cell lines were carefully detached by use of PBS containing 5 mM EDTA. No trypsin was used to avoid enzymatic cleavage of cell surface receptors.

* The costs of publication of this article were defrayed in part by the payment of page charges. This article must therefore be hereby marked "*advertisement*" in accordance with 18 U.S.C. Section 1734 solely to indicate this fact.

¶ Current address: Schering AG, Experimental Oncology, 13342 Berlin, Germany.

** To whom correspondence should be addressed. Tel.: 41-1-635-5570; Fax: 41-1-635-5712; E-mail: plueckthun@biocfebs.unizh.ch.

[1] The abbreviations used are: scFv, single-chain Fv fragment; AUC, area under curve; ECD, extracellular domain; ID/g, injected dose/g; RIA, radioimmunoassay; RU, response units; ^{99m}Tc, ^{99m}technetium; PBS, phosphate-buffered saline; BSA, bovine serum albumin; DOTA, 1,4,7,10-tetraazacyclodecane-*N*,*N*′,*N*″,*N*‴-tetraacetic acid.

The purified recombinant antigen p185^{HER-2}-ECD was a kind gift of Dr. Paul Carter (Genentech Inc., CA).

Cloning of Constructs—The scFv fragment of the human anti-p185^{HER-2} antibody 4D5 was constructed (19) from the Fab fragment (20) and had been used in several studies before (21–23). The 4D5-dhlx miniantibody construct was obtained by ligation of the *Eco*RI/*Hin*dIII fragment of the vector pKM30-dhlx-his (24), containing the dhlx sequence and the His tag, into the expression vector pIG6, containing the scFv fragment 4D5 (25). The nucleotide sequence for the p53 tetramerization domain was isolated as an *Eco*RI/*Asc*I fragment from the plasmid pACK9-9p53,[2] which contains the p53 tetramerization domain (26). The construct 4D5-p53 was then obtained by substituting the dhlx domain in the 4D5-dhlx construct by the *Eco*RI/*Asc*I fragment containing the p53 tetramerization domain.

Periplasmic Expression and Purification—All constructs were expressed in the periplasm of *E. coli* using the expression vector pIG6 under the control of a *lac* promoter (25). For large scale expression the constructs were transformed in the *E. coli* strain SB536 (27) and grown overnight. Twenty-five ml were then used for inoculation of 1 liter of 2YT medium containing 1% glucose and ampicillin (50 μg/ml) in a 5-liter baffled shake flask. The culture was grown at room temperature, and expression was induced with isopropyl-β-D-thiogalactopyranoside (Roche Molecular Biochemicals, 1 mM final concentration) for miniantibody production when it reached an $A_{550\ nm}$ of 0.5. Expression was continued for 3–4 h at 24 °C until the culture reached a final $A_{550\ nm}$ of 4–5. The harvested pellet was stored at −80 °C.

Briefly, the monomeric scFv fragment 4D5 was purified as described earlier (22). For purification of the miniantibodies 4D5-dhlx and 4D5-p53, the pellet of a 1-liter expression culture was resuspended in 50 ml of buffer containing 100 mM Tris (pH 7.0), 150 mM NaCl, 2 mM $MgCl_2$, 0.01% Tween 20, DNase (1 mg/100 ml), RNase (1 mg/100 ml). The cell suspension was lysed in two cycles with a French pressure cell press (SLS Instruments Inc., Urbana, IL), and to clear the lysate, it was centrifuged for 30 min in an SS-34-rotor at 48,000 × *g* at 4 °C. The protein was purified by a combination of immobilized metal ion affinity chromatography and ion exchange chromatography. Immobilized metal ion affinity chromatography purification of the 4D5-dhlx and 4D5-p53 was performed with a Ni^{2+}-iminodiacetic acid column on a BioCAD-system (PE Perseptive Biosystems). After loading of the lysate, the column was washed with 20 mM Tris (pH 7.0), 150 mM NaCl, 0.01% Tween 20 until the absorption reached the base line. The column was then washed with 20 mM Tris (pH 7.0), 1 M NaCl, 0.01% Tween 20 for 150 column volumes, followed by a further washing step with 80 mM imidazole, 20 mM Tris (pH 7.0), 150 mM NaCl for 40 column volumes. Proteins were then eluted with 500 mM imidazole (pH 7.0), 150 mM NaCl, and samples were collected in a fraction collector in tubes containing 100 mM Tris (pH 7.0), 8 mM EDTA for immediate 2-fold dilution. The collected sample was loaded on a HQ-Sepharose column (HQ 4.6/100) equilibrated with 2-fold diluted PBS. Impurities bound to the column, and the flow-through, containing the desired miniantibody, was collected and then dialyzed against PBS overnight at 4 °C, before it was concentrated to about 200–300 μg/ml by ultracentrifugation using Centricon micro-concentrators (Amersham Pharmacia Biotech).

Analytical Gel Filtration—Analytical gel filtration with non-labeled antibody fragments was performed on a SMART system (Amersham Pharmacia Biotech) using a Superose-12 column (PC3.2) equilibrated with degassed PBS containing 0.005% Tween 20. Thirty μl of the antibody fragments were injected at a concentration of 250 μg/ml. Analytical gel chromatography with radiolabeled antibody fragments was performed on a HiLoad system (Amersham Pharmacia Biotech). Either a Superose-12 (HR 10/30) column (Amersham Pharmacia Biotech) or a Superdex-200 (HR 10/30) column (Amersham Pharmacia Biotech), equilibrated in PBS containing 0.5% BSA, was used. For calibration of the Superose-12 column alcohol dehydrogenase (M_r 150,000), bovine serum albumin (M_r 66,000) and carbonic anhydrase (M_r 29,000) were used. The Superdex-200 column was calibrated with thyroglobulin (M_r 669,000), apoferritin (M_r 443,000), β-amylase (M_r 200,000), and alcohol-dehydrogenase (M_r 150,000).

His Tag-specific ^{99m}Tc Labeling of Antibody Fragments—^{99m}Tc labeling was carried out essentially as described before (23). To label the various constructs (200 μg/ml) they were mixed with the same volume of freshly prepared ^{99m}Tc-tricarbonyl (pH 6.8, 30 mCi to 1 Ci/ml) and incubated for 1 h at 37 °C. The reaction was stopped by removing the free ^{99m}Tc using a Biospin-6 column (Bio-Rad) equilibrated with PBS containing 0.005% Tween 20. The eluted fractions were quantitated for incorporated radioactivity by gamma-scintillation counting.

Determination of the Immunoreactive Fraction—The immunoreactive fraction of the antibody constructs on cells was determined as described by Lindmo *et al.* (28) and/or by gel filtration analysis. For the determination on cells, duplicate samples with increasing numbers of cells (0.5–10 × 10^6 cells/ml) were incubated in suspension with constant amounts (1–5 ng) of radiolabeled antibody fragments for 1 h at 4 °C on a shaker. Nonspecific binding was determined on control samples of cells, preincubated with a 100-fold excess of unlabeled antibody fragments in PBS containing 0.5% BSA for 1 h at 4 °C. Cells were washed three times with PBS containing 0.5% BSA, and the bound radioactivity in the cell pellets was determined by gamma-scintillation counting (28).

Alternatively, the immunoreactivity of the antibodies was determined by a gel filtration shift assay. After radiolabeling the constructs were separated from free ^{99m}Tc-tricarbonyl by gel filtration on a Superdex-200 (HR 10/30) column, equilibrated with PBS containing 0.5% BSA, on a HiLoad system (Amersham Pharmacia Biotech). The fraction containing the radiolabeled antibody fragment was identified by gamma-scintillation counting of the eluted fractions, and 10–20 ng of the radiolabeled antibody fragment were then incubated with a 100-fold molar excess of recombinant antigen p185^{HER-2}-ECD for 1 h at room temperature. After the binding equilibrium had been established, the sample was analyzed again on a second Superdex-200 (HR 10/30) column, and the eluted radioactivity in the collected fractions was monitored by gamma-scintillation counting and compared with the elution profile of the radiolabeled control antibody fragment not incubated with p185^{HER-2}-ECD antigen. Immunoreactivity was then estimated from the percentage of radioactivity eluting at higher molecular weight, indicating the formation of complexes of antigen and active radiolabeled antibody fragment.

Evaluation of Thermal and Serum Stability—The *in vitro* thermal and serum stability of the anti-p185^{HER-2}-antibody fragments was estimated in a gel filtration assay. After incubation at nanomolar concentration in human serum at 37 °C for 20 h radiolabeled antibody fragments were analyzed on a Superdex-200 (HR 10/30) column equilibrated in PBS containing 0.5% BSA. The elution profile of the radioactivity was then compared with the elution profile of the radiolabeled control antibody fragment diluted in PBS (containing 0.5% BSA) and stored at 4 °C. The loss of the peak with the desired molecular weight over time was examined.

Comparison of the Dissociation Kinetics of the Miniantibodies—A comparison of the dissociation kinetics of the various constructs was carried out by surface plasmon resonance by using a BIAcore instrument (Amersham Pharmacia Biotech), as well as on p185^{HER-2}-overexpressing SK-OV-3 cells. For the surface plasmon resonance measurements a CM5-Sepharose Chip (Amersham Pharmacia Biotech) was coated with 3000 RU p185^{HER-2}-ECD antigen by amine chemistry. Antibody fragments were injected in a volume of 30 μl on the coated surface and for estimation of nonspecific binding on an uncoated reference surface. The antibody concentration was chosen such that the surface was not saturated, and binding was about 50% of the maximally reachable RU values. The sensorgrams were obtained at a flow rate of 30 μl/min, and dissociation was followed for 6000 s. Data were evaluated with the BIAevaluation (3.0) software (Amersham Pharmacia Biotech).

Alternatively, dissociation of the miniantibodies was studied on cells overexpressing the p185^{HER-2} antigen. Duplicate samples of the radiolabeled 4D5 constructs were incubated with 0.5 × 10^6 SK-OV-3 cells suspended in 100 μl of PBS containing 0.5% BSA for 1 h at 4 °C. The cells were washed three times with PBS containing 0.5% BSA to remove initially unbound radioactivity and were then incubated at 37 °C on a shaker to start dissociation. Antibodies were used at non-saturating concentrations in which about 50% of maximum binding was reached (50% B_{max}). After 0, 5, 10, 15, 30, 60, 120, and 180 min, samples were taken and immediately washed three times with PBS containing 0.5% BSA to remove dissociated antibody fragments. When the last sample was taken, all samples were measured for the remaining radioactivity in a gamma-scintillation counter. For an estimation of nonspecifically bound radioactivity control samples were preincubated with a 100-fold excess of unlabeled antibody constructs for 1 h at 4 °C.

Determination of the Functional Affinity on SK-OV-3 Cells by Radioimmunoassay (RIA)—The functional affinity of the ^{99m}Tc-labeled anti-p185^{HER-2} antibody fragments on SK-OV-3 cells was determined by RIA. SK-OV-3-cells (0.5 × 10^6) were incubated with increasing amounts of the radiolabeled antibody fragments (50 pM to 30 nM) for 1 h at 4 °C, washed three times with PBS containing 0.5% BSA to remove unbound radioactivity, and measured for bound radioactivity in a gamma-scintillation counter. To correct for nonspecific binding, control samples

[2] P. Pack, unpublished data.

were preincubated with 100-fold excess of unlabeled antibody fragments for 1 h at 4 °C. All measurements were performed in duplicate. The corrected radioactivity was plotted against the scFv fragment concentration, and the functional affinity was calculated from the fit of the data, assuming a simple 1:1 model with the approximate function $y = y_{max} \cdot \times /(K_D + x)$, where x is the concentration of radioligand (corrected for activity); y is the radioactivity attributable to specific binding; and y_{max} is its plateau value.

Blood Clearance and Biodistribution—Blood clearance studies were performed in 6–8-week-old female Balb/c mice. Biodistribution analysis was carried out in athymic CD1 nu/nu mice (Charles River, Germany). For blood clearance studies each mouse received intravenous injections of 5–10 μg of radiolabeled antibody fragments (90–130 μCi/mouse). Mice were sacrificed after 7.5, 15, 30, 60, 120, and 180 min, and blood, liver, and kidney samples were taken and measured for radioactivity in a gamma-scintillation counter. The percentage of the injected dose/g tissue (% ID/g) was calculated for each time point. $t_{½}\alpha$ and $t_{½}\beta$ were obtained from the analysis of the plot of the % ID/g of the blood values over time with a biphasic exponential function (GraphPad software).

The serum stability of the multimeric miniantibodies in the circulation of Balb/c mice was examined by gel filtration of serum samples after administration of the radiolabeled constructs. Each mouse received intravenous injection of 100 μl of PBS containing 2–5 μg of radiolabeled antibody fragments. After 30 min mice were sacrificed, and blood samples were taken and centrifuged for 5 min at maximum speed in an Eppendorf lab centrifuge at room temperature. Then 150 μl of the serum was analyzed by gel filtration in PBS containing 0.5% BSA using a Superose-12 (HR10/30) column on a HiLoad system (Amersham Pharmacia Biotech). The eluted fractions were monitored in a gamma-scintillation counter for serum radioactivity. All data were normalized to the same amount of injected radioactivity (10×10^6 cpm).

Tumor localization studies of the ^{99m}Tc-labeled 4D5 antibody fragments were performed in nude mice xenografted with SK-OV-3 tumors. Tumors were raised subcutaneously at the lateral flanks by injections of 10^7 SK-OV-3 carcinoma cells in a total volume of 100 μl. Ten days after tumor inoculation, when tumors reached a size of 20–50 mm^3, each mouse received intravenous injections of 10–15 μg of radiolabeled miniantibody (1–2 mCi/mouse). The anti-fluorescein binding scFv fragment FITC-E2 (29) was used as a nonspecific control antibody. Mice were killed at 15 and 30 min and 1, 4, 24, 48, and 72 h after injection, and organs were removed, and radioactivity was measured in a gamma-scintillation counter. The areas under the curve (AUC) values were calculated with the GraphPad Software version 3.0 (GraphPad Software, San Diego CA).

RESULTS

Construction, Periplasmic Expression, and Purification of Multimeric Miniantibodies—The synthetic helix-turn-helix peptide dhlx (30) and the tetramerization peptide of the human tumor suppressor protein p53 were previously found to mediate the spontaneous di- and tetramerization of fused antibody fragments in the periplasm of *E. coli* to produce the so-called miniantibodies (6, 26, 31). We used these multimerization devices for the construction of di- and tetravalent miniantibodies of the anti-tumor anti-p185^{HER-2} antibody fragment 4D5 (19–22) (Fig. 1), expressed them in the periplasm of *E. coli,* and were able to purify them to greater than 95% purity (Fig. 2*A*). For the unmodified scFv fragment 4D5, we routinely obtained 1–2 mg/liter *E. coli* culture, whereas for the 4D5-dhlx and 4D5-p53 constructs 500 and ~250 μg/liter were obtained, respectively. Upon concentration by ultrafiltration, concentrations of 2–3 mg/ml could be obtained for the scFv 4D5, 400–500 μg/ml for the 4D5-dhlx miniantibody, and about 200–250 μg/ml for the 4D5-p53 tetrameric miniantibody.

Analysis of Multimer Formation—The occurrence of multimerization of the anti-p185^{HER-2} antibody fragments was demonstrated by gel filtration analysis of the purified proteins on a Superose-12 column (Fig. 2*B*). The unmodified scFv fragment 4D5 eluted at a retention volume of 1.56 ml as expected for a monomeric species. The 4D5-dhlx construct eluted at a volume of 1.43 ml, which corresponds to a calculated M_r of about 60,000 consistent with a dimer. The p53-multimerized species eluted at 1.32 ml, which corresponds to a calculated M_r of about

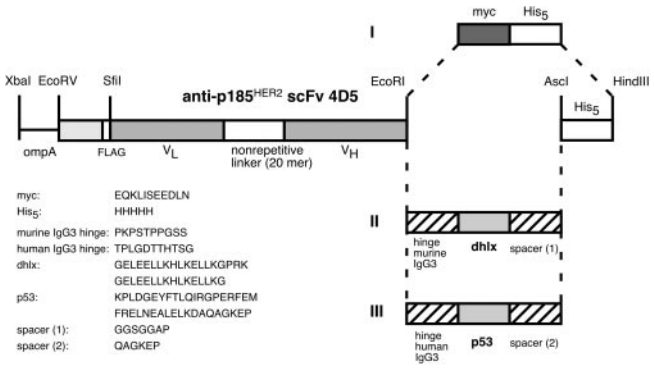

FIG. 1. **Construction scheme of multimerization of scFv 4D5 by self-associating peptides.** Shown are the *Xba*/*Hin*dIII cassettes of the expression vector pIG6 for production of the monomeric anti-p185^{HER-2} scFv (*I*), the di- (*II*), and tetrameric (*III*) miniantibodies in the bacterial periplasm. By simple exchange of the *Eco*RI/*Asc*I module one can easily switch between the molecular formats.

130,000 consistent with a tetramer. In no cases were higher molecular weight aggregates detected, and the elution of single symmetric peaks indicated the homogeneity of the protein preparations.

Efficiency of the His Tag-specific ^{99m}Tc Labeling—All 4D5 constructs could be labeled with ^{99m}Tc-tricarbonyl, which forms an extremely stable complex with clusters of histidine residues (23). No precipitate was observed in the reaction mixture. For the monomeric 4D5 about 70% of the free ^{99m}TcCO (which is present in molar trace amounts) was incorporated when the protein was used at 1 mg/ml. For the dimeric 4D5-dhlx usually 30% incorporation was obtained with an initial protein concentration of 500 μg/ml. To compare the data between the proteins of this study, all antibody fragments were used at concentrations of 250 μg/ml, which was the highest concentration achievable for the 4D5-p53 construct, and the routinely obtained incorporation yields of ^{99m}Tc-tricarbonyl were between 10 and 20% of the radionuclide (100–200 mCi/ml).

Immunoreactivity of the Multimers after Radiolabeling—To ensure the conservation of the binding activity of the multimers after radiolabeling, we measured the immunoreactivity of the constructs. In binding assays on SK-OV-3 cells we determined the immunoreactive fractions to be about 80–90% for the monomeric 4D5 scFv, above 95% for the 4D5-dhlx dimer, and 80% for the 4D5-p53 tetramer (Table I).

In a gel filtration shift assay (Table I), we found for scFv 4D5 and 4D5-dhlx that about 95% of the labeled molecules formed antigen complexes, whereas for 4D5-p53 about 55–60% of the radioactivity eluted earlier from the column than in the control experiment without antigen, indicating antigen complex formation. As the elution profiles comprised species of different stoichiometry, they were too complex to determine reliably the number of reactive binding sites (data not shown).

Thermal and Serum Stability of Radiolabeled Multimers—A sufficient stability of the antibody in serum and at high temperature is essential for tumor targeting (22). For this reason we compared the elution profile of ^{99m}Tc-labeled 4D5 constructs incubated in human serum at 37 °C and stored at 4 °C. For the unmodified 4D5 scFv fragment after serum incubation for 20 h around 50–60% of the protein still eluted at the volume expected for its respective molecular weight (13.5 ml), for the 4D5-dhlx construct 60% (12.2 ml), and for the 4D5-p53 90% (11.5 ml). These data indicate that the presence of the interaction domains does not increase aggregation and that the miniantibodies are at least as stable at 37 °C as the parent scFv, and possibly more.

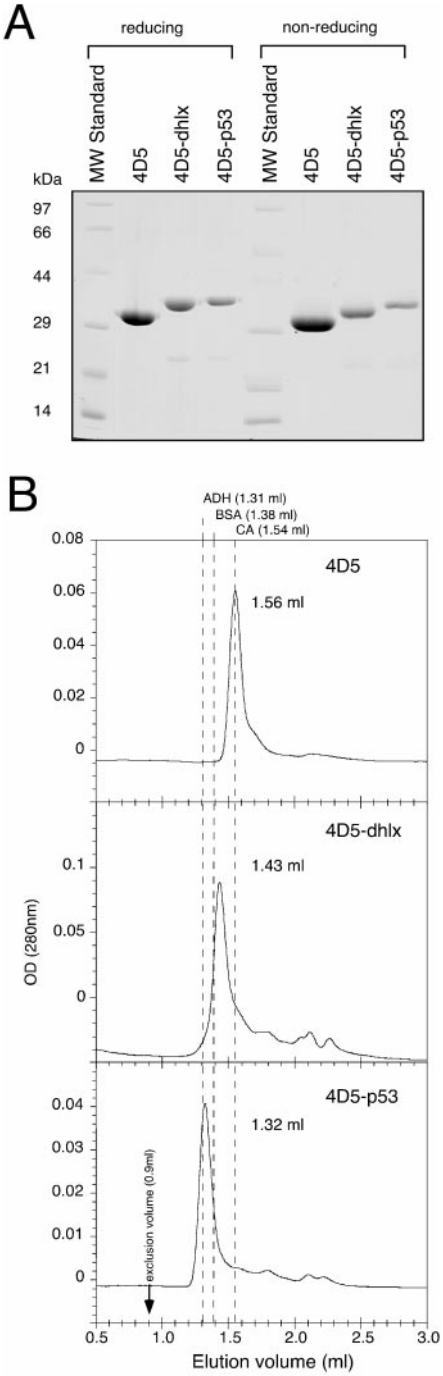

FIG. 2. *A,* purity of mono-, di-, and tetrameric anti-p185^{HER-2} antibody fragments. SDS-polyacrylamide gel electrophoresis under reducing and non-reducing conditions shows the result of the purification of the 4D5 scFv fragment and of the miniantibodies 4D5-dhlx and 4D5-p53. *B,* analysis of multimerization by size exclusion chromatography. *Top,* gel filtration analysis of unmodified 4D5 scFv fragment; *middle*, 4D5-dhlx; and *bottom,* 4D5-p53 on a Superose-12 column. Molecular weight standards are as follows: alcohol dehydrogenase (M_r 150,000); BSA (M_r 66,000); and carbonic anhydrase (*CA*, M_r 29,000).

Comparison of the Dissociation Kinetics of the Miniantibodies—To demonstrate the differences in the binding behavior due to the multimerization, we tested the dissociation kinetics of the various 4D5 constructs from their receptor both in surface plasmon resonance (BIAcore) experiments with purified p185^{HER-2} and on p185^{HER-2} overexpressing SK-OV-3 cells (Fig. 3).

For surface plasmon resonance (BIAcore) measurements, we coated the chip with high antigen densities to allow multivalent binding, which is not restricted by the distance between antigen molecules, but used high flow rates to minimize rebinding of dissociated molecules. Injected concentrations of the 4D5 constructs and the duration of the injection were chosen as to create a situation at the beginning of the off-rate measurements in which the binding surface was only saturated up to 50% of the maximum RU value, independently determined for each construct. The dissociation was followed for 100 min and revealed a slower dissociation for the 4D5-dhlx miniantibody (>92% after 100 min still bound to the receptor) and the 4D5-p53 miniantibody (85%) in comparison to the monomeric 4D5 scFv (58%). However, the observed dissociation for the dimeric 4D5 and the tetrameric 4D5 was similar and even slightly slower for the dimeric species.

In measurements performed on p185^{HER-2}-overexpressing SK-OV-3 cells, we found the unmodified 4D5 scFv to dissociate rapidly (65% bound after 100 min and 49% after 180 min), while bound 4D5-dhlx (76 and 63% after 100 and 180 min, respectively) and 4D5-p53 (73 and 60% after 100 and 180 min, respectively) dissociated more slowly. Again, the dissociation

TABLE I
Immunoreactivity of multimerized anti-p185^{HER-2}-antibody fragments

Antibody fragment	Immunoreactive fraction on cells[a]	Complex formation with p185^{HER-2}-ECD[a] determined by gel filtration
	%	
4D5-scFv	80–90	95
4D5-dhlx	>95	95
4D5-p53	80	55–60

[a] Immunoreactive fraction means binding to the antigen with at least one binding site.

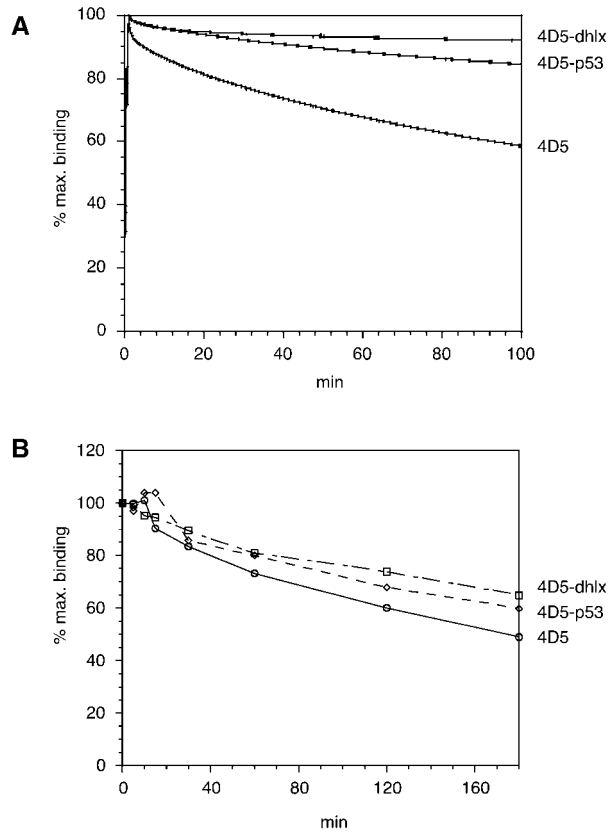

FIG. 3. **Increase in avidity by multimerization.** The increase of functional affinity obtained by multimerization was measured by surface plasmon resonance (BIAcore) on recombinant p185^{HER-2}-ECD (*A*) and on living SK-OV-3 cells overexpressing p185^{HER-2} (*B*).

TABLE II
Measurement of functional affinity of 4D5 constructs on SK-OV-3 cells

Antibody fragment	Functional affinity[a,b] on SK-OV-3 cells
	nM
4D5-scFv	9 ± 2
4D5-dhlx	2.9 ± 0.9
4D5-p53	3.3 ± 1

[a] The data were fitted to the simplified equation, $y = y_{max} \cdot x/(K_D + x)$, see "Materials and Methods," but only the data for the monomeric scFv fragment describe a thermodynamic affinity (K_D).
[b] Interaction was measured with ^{99m}Tc-labeled antibody constructs in a RIA format at 4 °C.

rates of 4D5-dhlx and the 4D5-p53 construct were very similar.

RIA Measurements of Functional Affinities on SK-OV-3 Cells—To complement the dissociation data, we also determined the equilibrium binding of the various constructs to p185^{HER-2}-overexpressing SK-OV-3 cells (Table II). An increase in functional affinity for the di- and tetramerized miniantibody was found in this cell line compared with the monomeric scFv 4D5. No significant difference in functional affinity (avidity) was found between di- and tetramer, however.

Blood Clearance and Biodistribution—The use of multimeric miniantibodies is expected to result in an increase in serum persistence. Therefore, we measured blood serum levels in clearance studies, and indeed we observed longer serum half-lives with increasing degree of multimerization (Fig. 4). The analysis of the obtained curves (Fig. 4*A*) yielded for the monomeric 4D5 a $t_{1/2}\alpha$ = 1 min and $t_{1/2}\beta$ = 0.34 h, for the 4D5-dhlx a $t_{1/2}\alpha$ = 2.05 min and $t_{1/2}\beta$ = 0.54 h, and for the 4D5-p53 a $t_{1/2}\alpha$ = 7 min and $t_{1/2}\beta$ = 2.18 h.

The gel filtration analysis of serum samples taken from the circulation 30 min after injection (Fig. 4*B*) shows that the various species are stable with respect to their multimerization, as no other peaks were observed, and they are cleared with different rates from the circulation, since the levels dropped at different rates. No peaks originating from dissociated multimers were observed, probably because such species would not accumulate, as they are rapidly cleared.

To analyze the tumor targeting potential of the various constructs, we performed biodistribution studies in xenografted nude mice (Table III). The monomeric scFv 4D5 enriched to 1.1% ID/g in SK-OV-3 tumors with a tumor-to-blood ratio of 6.5. This is consistent with results of earlier targeting experiments with this scFv fragment (23). After 48 h, 0.98% ID/g and a tumor-to-blood ratio of 13.5 were found. The dimeric miniantibody 4D5-dhlx accumulated at the tumor site with 1.47% ID/g after 24 h with a tumor-to-blood ratio of 7, and it followed the same kinetics as the monomeric scFv 4D5. Dimerization of the scFv 4D5 by the dhlx domain and formation of a dimeric miniantibody thus did not lead to a significant improvement (Table III). In contrast, an improved selectivity and an increased total dose enrichment was obtained with the tetrameric 4D5-p53 construct. After 24 h 4.32% ID/g was accumulated at the tumor site with a tumor-to-blood ratio of 3.4, and the antibody fragment remained stably bound, since after 48 h 3.24% ID/g tissue was still present at the tumor with a tumor-to-blood ratio of 13.5. Regarding the residence time at the tumor the tetrameric 4D5-p53 construct was the most efficient with a total calculated AUC value of 10,270 after 48 h and 13,400 after 72 h. For the monomeric 4D5 an AUC value of 3285 was calculated after 48 h, and for the dimeric 4D5-dhlx values of 3573 (48 h) and of 4380 (72 h) were calculated.

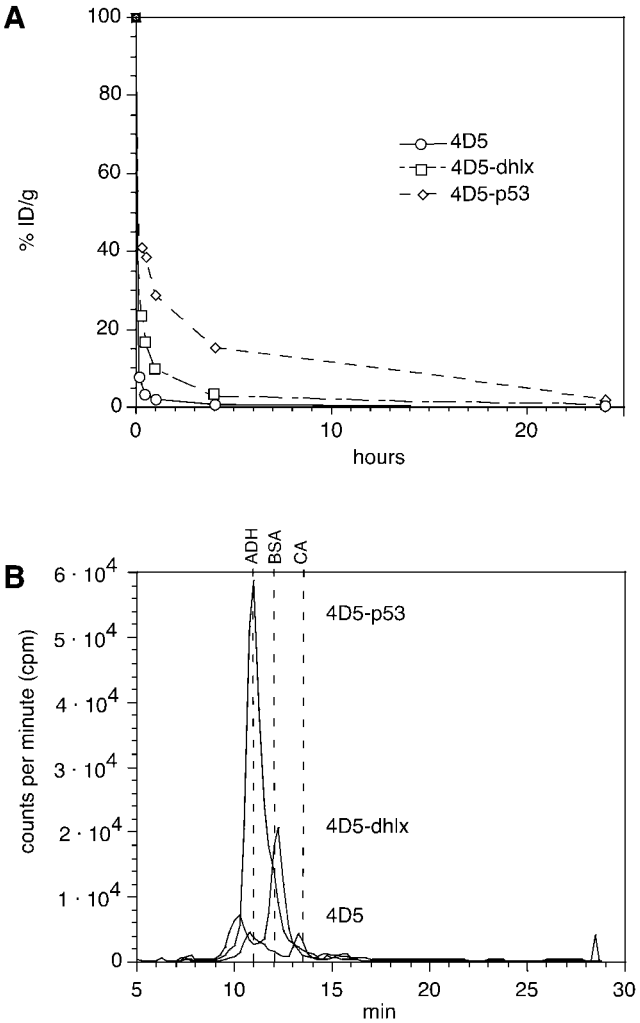

FIG. 4. **Influence of multimerization on the clearance of 4D5 antibody fragments.** *A,* blood clearance was examined in Balb/c mice and followed over 24 h. *B,* serum samples were taken from sacrificed mice 30 min after injection and analyzed by size exclusion chromatography on a Superose-12 column. Each mouse received the same amount of antibody fragment, and the measured radioactivity was normalized to 10×10^6 cpm.

DISCUSSION

Two aspects of multimerization are of importance for efficient tumor targeting as follows: (i) multimerization leads to higher functional affinity by increasing the number of binding sites, and (ii) the molecular weight is automatically increased by the presence of multiple copies of the binding domains. This higher molecular weight extends the serum persistence of molecules in the circulation, because they are not filtrated into the kidney glomeruli (4, 9, 32). For molecules that are too large to pass this filtration barrier, the blood pool remains at a high concentration level over time, and thus there is a higher chance for these molecules to bind to their target antigens. On the other hand, there is an inverse correlation between the molecular weight of these molecules and their ability to penetrate into the tumor tissue. To overcome this drawback a compromise has to be found in the design of the targeting molecules with respect to the molecular weight. Because of the conflicting nature of these requirements the optimal molecular design can only be determined experimentally.

In the present study we report the production and the *in vitro* and *in vivo* properties of mono-, di-, and tetramerized anti-p185^{HER-2} scFv fragments in the format of miniantibodies. Multimerization was achieved by the use of self-associating

TABLE III
Biodistribution of ^{99m}Tc-labeled scFv fragments in athymic mice bearing SK-OV3 tumor xenografts

Antibody	Organ	15 min	30 min	1 h	4 h	24 h	48 h	72 h
4D5[a,b]	Blood	4.5 ± 1.53		0.87 ± 0.12	0.47 ± 0.11	0.16 ± 0.04	0.07 ± 0.02	
	Heart	2.42 ± 0.72		0.56 ± 0.08	0.41 ± 0.1	0.28 ± 0.12	0.15 ± 0.01	
	Lung	2.86 ± 0.4		0.79 ± 0.07	0.55 ± 0.15	0.29 ± 0.07	0.15 ± 0.00	
	Spleen	1.69 ± 0.24		0.79 ± 0.16	0.8 ± 0.22	0.67 ± 0.28	0.34 ± 0.16	
	Kidney	170 ± 27		211 ± 15	206 ± 41	119 ± 19	72 ± 10	
	Stomach	0.93 ± 0.28		0.49 ± 0.19	0.5 ± 0.07	0.31 ± 0.02	0.12 ± 0.07	
	Intestine	1.27 ± 0.37		0.47 ± 0.1	0.48 ± 0.01	0.31 ± 0.09	0.12 ± 0.02	
	Liver	2.64 ± 0.72		2.01 ± 0.28	2.38 ± 0.67	2.29 ± 0.8	1.26 ± 0.15	
	Muscle	0.77 ± 0.24		0.25 ± 0.03	0.2 ± 0.01	0.2 ± 0.04	0.08 ± 0.02	
	Bone	0.59 ± 0.44		0.49 ± 0.43	0.29 ± 0.19	0.16 ± 0.11	0.09 ± 0.07	
	Tumor	1.56 ± 0.31		1.06 ± 0.19	1.55 ± 0.26	1.04 ± 0.15	0.94 ± 0.26	
	Tumor:Blood ratio[c]	0.34		1.2	3.3	6.5	13.4	
4D5-dhlx[a,b]	Blood		12.97 ± 1.68		1.4 ± 0.36	0.21 ± 0.01	0.09 ± 0.02	0.02 ± 0.01
	Heart		6.11 ± 1.17		1.99 ± 0.28	1.57 ± 0.52	0.79 ± 0.22	0.58 ± 0.03
	Lung		7.3 ± 1.01		2.64 ± 1.79	0.81 ± 0.22	0.46 ± 0.08	0.25 ± 0.03
	Spleen		6.4 ± 1.35		7.5 ± 3.62	5.8 ± 1.48	3.7 ± 2.38	3.5 ± 2.85
	Kidney		69 ± 49		99 ± 18	63 ± 8	43 ± 5	26 ± 7
	Stomach		1.17 ± 0.56		1.09 ± 0.55	0.4 ± 0.34	0.4 ± 0.13	0.25 ± 0.01
	Intestine		1.71 ± 0.35		1.68 ± 0.37	1.05 ± 0.14	0.68 ± 0.2	0.4 ± 0.08
	Liver		10.5 ± 0.95		8.4 ± 2.56	7.0 ± 0.89	5.4 ± 1.65	2.9 ± 0.56
	Muscle		0.55 ± 0.16		0.34 ± 0.08	0.28 ± 0.09	0.15 ± 0.01	0.02 ± 0.01
	Bone		1.31 ± 0.97		1.55 ± 1.55	0.81 ± 0.61	0.45 ± 0.41	0.65 ± 0.51
	Tumor		0.85 ± 0.37		1.61 ± 0.61	1.47 ± 0.6	0.55 ± 0.06	0.57 ± 0.41
	Tumor:Blood ratio[c]		0.06		1.15	7	6.1	28.5
4D5-p53[a,b]	Blood		28.7 ± 3.18	25.1 ± 7.17	11.4 ± 1.52	1.28 ± 0.45	0.24 ± 0.06	0.07 ± 0.02
	Heart		11.9 ± 3.1	12.0 ± 4.0	6 ± 0.5	2.1 ± 0.3	1.5 ± 0.49	1.0 ± 0.2
	Lung		13.6 ± 1.16	13.5 ± 1.96	6.2 ± 0.48	1.83 ± 0.42	0.99 ± 0.03	0.58 ± 0.06
	Spleen		6.8 ± 0.87	6.9 ± 1.52	4.4 ± 0.78	3.6 ± 0.23	2.9 ± 1.08	3.2 ± 0.78
	Kidney		33 ± 4	42 ± 6	68 ± 3	63 ± 9	40 ± 7	28 ± 1
	Stomach		1.06 ± 0.4	2.1 ± 0.73	1.29 ± 0.4	0.94 ± 0.12	0.53 ± 0.24	0.37 ± 0.19
	Intestine		2.54 ± 0.23	3.1 ± 0.75	2.04 ± 0.02	1.14 ± 0.12	0.72 ± 0.11	0.48 ± 0.11
	Liver		9.7 ± 1.49	9.8 ± 2.28	8.1 ± 0.43	7.4 ± 1.04	6.1 ± 1.68	4.2 ± 0.05
	Muscle		0.79 ± 0.16	0.8 ± 0.22	0.58 ± 0.13	0.75 ± 0.22	0.38 ± 0.1	0.31 ± 0.3
	Bone		1.69 ± 1.24	2.3 ± 1.91	1.18 ± 0.94	0.88 ± 0.66	0.67 ± 0.52	0.50 ± 0.2
	Tumor		1.2 ± 0.06	1.95 ± 0.2	2.89 ± 0.25	4.32 ± 1.94	3.24 ± 0.85	1.11 ± 1.31
	Tumor:Blood ratio[c]		0.04	0.08	0.25	3.37	13.5	15.85
FITC-E[a,b]	Blood				0.58 ± 0.15	0.18 ± 0.03		
	Heart				0.37 ± 0.15	0.16 ± 0.02		
	Lung				0.54 ± 0.08	0.24 ± 0.03		
	Spleen				0.35 ± 0.03	0.24 ± 0.05		
	Kidney				153 ± 4	114 ± 15		
	Stomach				0.7 ± 0.74	0.24 ± 0.15		
	Intestine				0.4 ± 0.08	0.23 ± 0.05		
	Liver				1.51 ± 0.42	1.24 ± 0.18		
	Muscle				0.15 ± 0.01	0.11 ± 0.02		
	Bone				0.21 ± 0.14	0.11 ± 0.06		
	Tumor				0.73 ± 0.19	0.31 ± 0.1		
	Tumor:Blood ratio[c]				1.26	1.72		

[a] Biodistribution of ^{99m}Tc-labeled antibody fragments was studied in athymic mice ($n = 3$) bearing SK-OV-3 tumors of 20–50 mg in size after intravenous injection of the radiolabeled antibodies.
[b] Data are injected dose per g tissue (% ID/g) and were expressed as the mean ± S.E.
[c] The ratios presented are the averages of the tumor:blood ratios for the individual mice.

peptides (31), which lead to spontaneous assembly of the fused antibody fragments directly in the periplasm of *E. coli* (Fig. 1). The multimeric antibody fragments could be expressed and purified in good yields from *E. coli* as native proteins without refolding (Fig. 2*A*). The degree of multimerization was checked by gel chromatography analysis, and the presence of the expected mono-, di-, and tetrameric species was confirmed (Fig. 2*B*). The anti-p185^{HER-2} (anti-c-*erb*B2) 4D5 scFv fragment was chosen for this study, because it was reported to be of high affinity (20), above average equilibrium thermodynamic (21) and thermal stability (22), and could be purified in high yields from the periplasm of *E. coli* (19, 33). Furthermore, we have shown that the 4D5 scFv fragment could be labeled by His tag-specific ^{99m}Tc labeling to high specific activities and that it sufficiently localizes to SK-OV-3 xenografts in nude mice (23). Our expectation was that this antibody fragment confers favorable biophysical properties to the miniantibodies and that the effect of multimerization by the self-associating peptides on the overall integrity of the miniantibody and its tumor targeting properties could be studied without limitation by the antibody fragment used. Experimental analysis indeed showed that the thermal and serum stability, which are important prerequisites for efficient targeting, were retained during multimerization and not lost in the miniantibody formats.

The binding behavior was analyzed on immobilized recombinant p185^{HER-2}-ECD in BIAcore experiments and on p185^{HER-2}-overexpressing cells. In both experiments di- and tetrameric 4D5 miniantibodies showed a reduced dissociation rate compared with the monomeric 4D5 scFv, and this was undoubtedly due to the increased avidity of these molecules. Nevertheless, in none of the experiments 4D5-p53 exhibited a slower dissociation than the 4D5-dhlx construct. A dissociation of the tetramer into dimers seems to be unlikely, since it has been demonstrated that the tetramer still exists at the nanomolar concentrations used (Fig. 3). From the binding experiments and the RIA-measurements (Table II), we conclude that in targeting the 4D5 epitope on SK-OV-3 cells not more than two antigen-binding sites could be simultaneously engaged. However, this result can certainly not be generalized, as the avidity effect of going from a dimer to a tetramer will depend on

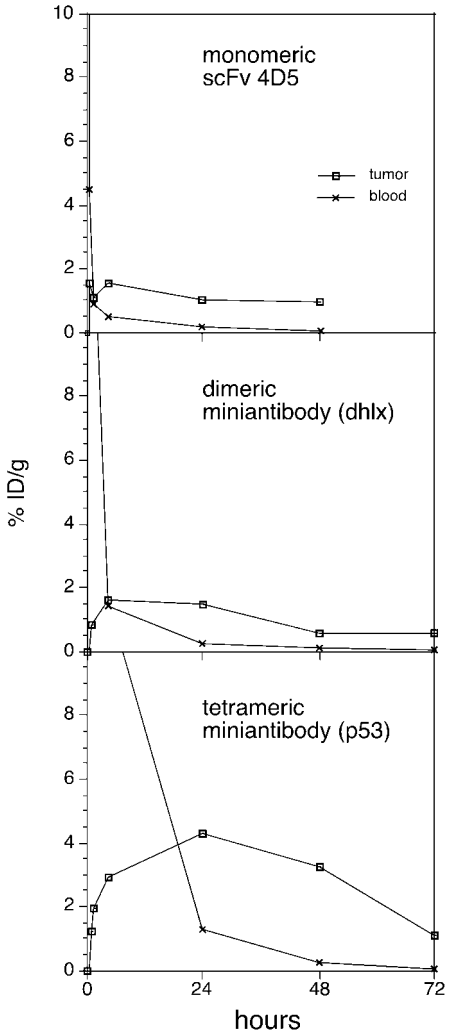

FIG. 5. **Tumor enrichment of mono-, di-, and tetrameric anti-p185^{HER-2} antibody fragments.** Each mouse received intravenously 10–15 μg of ^{99m}Tc-labeled 4D5 antibody fragments. Mice (n = 3 per time point) were sacrificed after 15 and 30 min and 1, 4, 24, 48, and 72 h. Tumor and blood samples were taken, measured for radioactivity, and the % ID/g was calculated.

the geometric orientation of the targeted epitope, its surface density, its accessibility, and the concentration of the multimer. In a previous study mono-, di-, and tetrameric anti-Lewis^{Y} scFv constructs were tested in a similar experiment, and increased avidity was found with increasing number of binding sites (26).

In clearance studies we found longer serum persistence with an increasing degree of multimerization (Fig. 4). Analysis of serum samples 30 min after intravenous injection showed stable multimerization of all miniantibody constructs. In biodistribution experiments in tumor xenografted nude mice, we monitored the organ and tumor distribution over a period of 72 h (Table III) and observed that the dimeric 4D5-dhlx construct did not show any significant improvement in tumor localization, compared with the monomeric scFv 4D5, despite its higher avidity. Although the 4D5-dhlx miniantibody cleared more slowly from the circulation than the monomeric scFv 4D5, its clearance rate was still faster than that of a well localizing iodinated diabody used in a recent study (14). The dissociation constants for the dhlx and p53 module into monomeric constituents are not known, and we cannot exclude that, at the high dilution in the serum, the non-covalent dimerization provided by the dhlx domain may slowly dissociate over time, leading to insufficient serum persistence and poorer tumor localization. As a consequence, the avidity gain by dimerization of molecules not yet bound could also be slowly lost under these conditions. The 4D5-p53 construct, on the other hand, was the most efficient in terms of tumor localization. Due to its tetrameric nature this 130-kDa molecule was above the renal threshold and showed the slowest clearance rate. The optimal time point for 4D5-p53 localization was reached only after 48 h with a 6-fold higher tumor localization than the dimeric construct and a tumor-to-blood ratio of 13.5:1 (Table III and Fig. 5). To our knowledge no ^{99m}Tc-biodistribution study for the 4D5 monoclonal antibody was reported so that we cannot directly compare it to the tetramer. However, the radiometal-labeled DOTA-conjugated anti-HER2/neu antibody 4D5 accumulated in nude mice with high total dose in transfected MCF7/HER2 tumor xenografts, but at no time point were tumor-to-blood ratios better than 2.6 obtained (34).

In summary, our results show that miniantibodies multimerized by self-associating peptides in the periplasm of *E. coli* have the potential to localize efficiently to tumor xenografts *in vivo* and to remain stably bound to their target antigen. This is the first study investigating the *in vivo* performance of this approach, and it has several consequences for the further development of these molecules in the future. From the two types of modules tested the tetrameric miniantibody was suitable to obtain significant tumor-to-blood ratios and efficient tumor localization. Nevertheless, it appears that the multimerization modules investigated dissociate over a time course of 72 h. This is not surprising, given the fact that they are held together by non-covalent forces and were highly diluted after injection into the animals, whereas they were at micromolar concentrations during the radiolabeling step, such that the oligomeric molecule was maintained at equilibrium. Further variants of these domains may help to better address this issue, either by evolving high affinity domains (35) and/or by introducing disulfide bonds (36). The final format will not only have to provide stability against dissociation, but should also result in facile production, which at least for the disulfide-bridged molecules is usually less favorable, and some formats even have to be made in eukaryotes (7). For non-covalent diabodies some dissociation would be expected as well over time, but to our knowledge this has not yet been determined.

The advantage of the self-associating peptides is that they allow a modular engineering approach in which it is possible to switch from one format to the other depending on the aim of the *in vivo* application. The approach is also completely general, as it does not depend on the details of the heavy chain variable domain/light chain variable domain interface and can be used for the multimerization of modules other than antibody fragments as well. Moreover, the self-associating peptides will allow the production of recombinant proteins containing additional effector domains with the smallest possible size in the periplasm of *E. coli*. Such developments are potentially of great significance for the development of novel and more effective targeting strategies in cancer therapy.

Acknowledgments—We thank Dr. Paul Carter for the gift of p185^{HER-2}-ECD, Christine de Pasquale for excellent technical assistance, and Drs. Ilse Novak-Hofer and Alain Tissot for helpful discussions.

REFERENCES

1. Holliger, P., and Hoogenboom, H. (1998) *Nat. Biotechnol.* **16,** 1015–1016
2. Begent, R. H., Verhaar, M. J., Chester, K. A., Casey, J. L., Green, A. J., Napier, M. P., Hope-Stone, L. D., Cushen, N., Keep, P. A., Johnson, C. J., Hawkins, R. E., Hilson, A. J., and Robson, L. (1996) *Nat. Med.* **2,** 979–984
3. Adams, G. P., Schier, R., Marshall, K., Wolf, E. J., McCall, A. M., Marks, J. D., and Weiner, L. M. (1998) *Cancer Res.* **58,** 485–490
4. Rowlinson-Busza, G. (1996) *Tumor Targeting* **2,** 37–48
5. Hudson, P. J. (1999) *Curr. Opin. Immunol.* **11,** 548–557
6. Plückthun, A., and Pack, P. (1997) *Immunotechnology* **3,** 83–105
7. Hu, S., Shively, L., Raubitschek, A., Sherman, M., Williams, L. E., Wong, J. Y.,

Shively, J. E., and Wu, A. M. (1996) *Cancer Res.* **56,** 3055–3061
8. Werlen, R. C., Lankinen, M., Offord, R. E., Schubiger, P. A., Smith, A., and Rose, K. (1996) *Cancer Res.* **56,** 809–815
9. King, D. J., Turner, A., Farnsworth, A. P., Adair, J. R., Owens, R. J., Pedley, R. B., Baldock, D., Proudfoot, K. A., Lawson, A. D., and Beeley, N. R. (1994) *Cancer Res.* **54,** 6176–6185
10. Casey, J. L., King, D. J., Chaplin, L. C., Haines, A. M., Pedley, R. B., Mountain, A., Yarranton, G. T., and Begent, R. H. (1996) *Br. J. Cancer* **74,** 1397–1405
11. Huston, J. S., Adams, G. P., McCartney, J. E., Tai, M. S., Hudziak, R. M., Oppermann, H., Stafford, W. F., III, Liu, S., Fand, I., and Apell, G. (1994) *Cell Biophys.* **25,** 267–78
12. Adams, G. P., McCartney, J. E., Tai, M. S., Oppermann, H., Huston, J. S., Stafford, W. F. D., Bookman, M. A., Fand, I., Houston, L. L., and Weiner, L. M. (1993) *Cancer Res.* **53,** 4026–4034
13. Holliger, P., and Winter, G. (1997) *Cancer Immunol. Immunother.* **45,** 128–130
14. Adams, G. P., Schier, R., McCall, A. M., Crawford, R. S., Wolf, E. J., Weiner, L. M., and Marks, J. D. (1998) *Br. J. Cancer* **77,** 1405–1412
15. Viti, F., Tarli, L., Giovannoni, L., Zardi, L., and Neri, D. (1999) *Cancer Res.* **59,** 347–352
16. Plückthun, A., Krebber, A., Krebber, C., Horn, U., Knüpfer, U., Wenderoth, R., Nieba, L., Proba, K., and Riesenberg, D. (1996) in *Antibody Engineering, A Practical Approach* (McCafferty, J., Hoogenboom, H. R., and Chiswell, D. J., eds) pp. 203–252, IRL Press, Oxford.
17. Pack, P., Kujau, M., Schroeckh, V., Knüpfer, U., Wenderoth, R., Riesenberg, D., and Plückthun, A. (1993) *Bio/Technology* **11,** 1271–1277
18. Horn, U., Strittmatter, W., Krebber, A., Knüpfer, U., Kujau, M., Wenderoth, R., Müller, K., Matzku, S., Plückthun, A., and Riesenberg, D. (1996) *Appl. Microbiol. Biotechnol.* **46,** 524–532
19. Knappik, A., and Plückthun, A. (1995) *Protein Eng.* **8,** 81–89
20. Carter, P., Presta, L., Gorman, C. M., Ridgway, J. B., Henner, D., Wong, W. L., Rowland, A. M., Kotts, C., Carver, M. E., and Shepard, H. M. (1992) *Proc. Natl. Acad. Sci. U. S. A.* **89,** 4285–4289
21. Wörn, A., and Plückthun, A. (1998) *FEBS Lett.* **427,** 357–361
22. Willuda, J., Honegger, A., Waibel, R., Schubiger, P. A., Stahel, R., Zangemeister-Wittke, U., and Plückthun, A. (1999) *Cancer Res.* **59,** 5758–5767
23. Waibel, R., Alberto, R., Willuda, J., Finnern, R., Schibli, R., Stichelberger, A., Egli, A., Abram, U., Mach, J. P., Plückthun, A., and Schubiger, P. A. (1999) *Nat. Biotechnol.* **17,** 897–901
24. Müller, K. M., Arndt, K. M., and Plückthun, A. (1998) *FEBS Lett.* **432,** 45–49
25. Ge, L., Knappik, A., Pack, P., Freund, C., and Plückthun, A. (1995) in *Antibody Engineering* (Borrebaeck, C. A. K., ed) 2nd Ed., pp. 229–261, Oxford University Press, Oxford
26. Rheinnecker, M., Hardt, C., Ilag, L. L., Kufer, P., Gruber, R., Hoess, A., Lupas, A., Rottenberger, C., Plückthun, A., and Pack, P. (1996) *J. Immunol.* **157,** 2989–2997
27. Bass, S., Gu, Q., and Christen, A. (1996) *J. Bacteriol.* **178,** 1154–1161
28. Lindmo, T., Boven, E., Cuttitta, F., Fedorko, J., and Bunn, P. A., Jr. (1984) *J. Immunol. Methods* **72,** 77–89
29. Vaughan, T. J., Williams, A. J., Pritchard, K., Osbourn, J. K., Pope, A. R., Earnshaw, J. C., McCafferty, J., Hodits, R. A., Wilton, J., and Johnson, K. S. (1996) *Nat. Biotechnol.* **14,** 309–314
30. O'Shea, E. K., Rutkowski, R., and Kim, P. S. (1989) *Science* **243,** 538–542
31. Pack, P., and Plückthun, A. (1992) *Biochemistry* **31,** 1579–1584
32. Behr, T. M., Goldenberg, D. M., and Becker, W. (1998) *Eur. J. Nucl. Med.* **25,** 201–212
33. Carter, P., Kelley, R. F., Rodrigues, M. L., Snedecor, B., Covarrubias, M., Velligan, M. D., Wong, W. L., Rowland, A. M., Kotts, C. E., and Carver, M. E. (1992) *Bio/Technology* **10,** 163–167
34. Tsai, S. W., Sun, Y. Y., Williams, L. E., Raubitschek, A. A., Wu, A. M., and Shively, J. E. (2000) *Bioconjugate Chem.* **11,** 327–334
35. Arndt, K. M., Pelletier, J. N., Müller, K. M., Alber, T., Michnick, S. W., and Plückthun, A. (2000) *J. Mol. Biol.* **295,** 627–639
36. Bloemendal, H. J., Logtenberg, T., and Voest, E. E. (1999) *Eur. J. Clin. Invest.* **29,** 802–809